World Journal of Radiology

Submit a Manuscript: https://www.f6publishing.com

*World J Radiol* 2019 June 28; 11(6): 81-93

DOI: 10.4329/wjr.v11.i6.81

ISSN 1949-8470 (online)

ORIGINAL ARTICLE

Retrospective Cohort Study

# Positron emission tomography/computed tomography imaging appearance of benign and classic "do not touch" osseous lesions

Stacey M Elangovan, Ronnie Sebro

**ORCID number:** Stacey M Elangovan (0000-0001-5359-9115); Ronnie Sebro (0000-0001-7232-4416).

**Author contributions:** Elangovan SM and Sebro R designed and performed the research and wrote the paper; Sebro R analyzed the data.

**Institutional review board statement:** The study was reviewed and approved by the local institutional review board and the need for signed informed consent for each participant was waived.

**Informed consent statement:** The study was reviewed and approved by the local institutional review board and the need for signed informed consent for each participant was waived.

**Conflict-of-interest statement:** The authors declare no conflicts of interest

**Data sharing statement:** Data available upon request from the senior author.

**STROBE statement:** The manuscript was prepared and revised according to the STROBE Statement-checklist of items.



**Stacey M Elangovan, Ronnie Sebro,** Department of Radiology, University of Pennsylvania, Philadelphia, PA 19104, United States

**Ronnie Sebro,** Department of Orthopedic Surgery, University of Pennsylvania, Philadelphia, PA 19104, United States

**Ronnie Sebro,** Department of Genetics, University of Pennsylvania, Philadelphia, PA 19104, United States

**Ronnie Sebro,** Department of Biostatistics, Epidemiology and Informatics, University of Pennsylvania, Philadelphia, PA 19104, United States

**Corresponding author:** Ronnie Sebro, MD, PhD, Assistant Professor, Department of Radiology, University of Pennsylvania, 3400 Spruce Street, Philadelphia, PA 19104, United States. ronnie.sebro@uphs.upenn.edu
**Telephone:** +1-215-2949512
**Fax:** +1-215-6153316

## Abstract

### *BACKGROUND*

Classic "do not touch" and benign osseous lesions are sometimes detected on $^{18}$-F-fluorodeoxyglucose ($^{18}$F-FDG) positron emission tomography/computed tomography (PET/CT) studies. These lesions are often referred for biopsy because the physician interpreting the PET/CT may not be familiar with the spectrum of $^{18}$F-FDG uptake patterns that these lesions display.

### *AIM*

To show that "do not touch" and benign osseous lesions can have increased $^{18}$F-FDG uptake above blood-pool on PET/CT; therefore, the CT appearance of these lesions should dictate management rather than the standardized uptake values (SUV).

### *METHODS*

This retrospective study evaluated 287 independent patients with 287 classic "do not touch" (benign cystic lesions, insufficiency fractures, bone islands, bone infarcts) or benign osseous lesions (hemangiomas, enchondromas, osteochondromas, fibrous dysplasia, Paget's disease, osteomyelitis) who underwent $^{18}$F-FDG positron emission tomography/computed tomography (PET/CT) at a tertiary academic healthcare institution between 01/01/2006 and 12/1/2018. The maximum and mean SUV, and the ratio of the maximum SUV to mean blood pool were calculated. Pearson's correlations between lesion size and

**Manuscript source**: Unsolicited manuscript

**Received:** March 7, 2019
**Peer-review started:** March 11, 2019
**First decision:** April 16, 2019
**Revised:** May 11, 2019
**Accepted:** June 20, 2019
**Article in press:** June 21, 2019
**Published online:** June 28, 2019

**P-Reviewer:** Bazeed M, Gao BL
**S-Editor:** Dou Y
**L-Editor:** A
**E-Editor:** Ma YJ

maximum SUV were calculated.

*RESULTS*

The ranges of the maximum SUV were as follows: For hemangiomas (0.95-2.99), bone infarcts (0.37-3.44), bone islands (0.26-3.29), enchondromas (0.46-2.69), fibrous dysplasia (0.78-18.63), osteochondromas (1.11-2.56), Paget's disease of bone (0.93-5.65), insufficiency fractures (1.06-12.97) and for osteomyelitis (2.57-12.64). The range of the maximum SUV was lowest for osteochondromas (maximum SUV 2.56) and was highest for fibrous dysplasia (maximum SUV of 18.63). There was at least one lesion that demonstrated greater $^{18}$F-FDG avidity than the blood pool amongst each lesion type, with the highest maximum SUV ranging from 9.34 times blood pool mean (osteomyelitis) to 1.42 times blood pool mean (hemangiomas). There was no correlation between the maximum SUV and the lesion size except for enchondromas. Larger enchondromas had higher maximum SUV ($r$ = 0.36, $P$ = 0.02).

*CONCLUSION*

The classic "do not touch" lesions and classic benign lesions can be $^{18}$F-FDG avid. The CT appearance of these lesions should dictate clinical management rather than the maximum SUV.

**Key words:** Positron emission tomography/computed tomography; Skeletal-axial; Skeletal-appendicular; "Do not touch" lesions



**Core tip:** Several benign and "do not touch" osseous lesions have $^{18}$F-FDG uptake above blood pool. Clinical management should be based on the CT appearance of these lesions rather than the maximum SUV uptake from PET/CT.

**Citation:** Elangovan SM, Sebro R. Positron emission tomography/computed tomography imaging appearance of benign and classic "do not touch" osseous lesions. *World J Radiol* 2019; 11(6): 81-93
**URL**: https://www.wjgnet.com/1949-8470/full/v11/i6/81.htm
**DOI**: https://dx.doi.org/10.4329/wjr.v11.i6.81

## INTRODUCTION

$^{18}$F-Fluorodeoxyglucose ($^{18}$F-FDG) positron emission tomography/computed tomography (PET/CT) is increasingly utilized for staging and surveillance of many common malignancies[1,2]. Approximately 1.9 million $^{18}$F-FDG PET/CT studies were performed in the United States in 2017, a 13% increase compared to 2015[3]. Cancer cells often switch from oxidative to glucose metabolism, even in the presence of oxygen, resulting in aerobic glycolysis[4], first described by Warburg[5,6]. This change in cancer cell metabolism is easily detected and measured in vivo using $^{18}$F-FDG PET/CT[3]. The rapid rise in the number of $^{18}$F-FDG PET/CT scans performed annually has the potential to increase the number of incidental findings[7-9]. Simultaneously, there has been increased specialization of radiology with most physicians that interpret $^{18}$F-FDG PET/CT not being simultaneously fellowship-trained in musculoskeletal radiology[10-14].

As a result, incidentally detected $^{18}$F-FDG-avid osseous lesions are often subject to sometimes inappropriate clinical management. A previous meta-analysis showed that although a general approach to $^{18}$F-FDG-avid incidental lesions may be recommended for selected organ systems, osseous lesions remain less amenable to blanket recommendations for or against biopsy, for incidentally noted $^{18}$F-FDG-avid osseous lesions[15]. Anecdotally, we have noted a concomitant increase in request for biopsies of incidentally noted $^{18}$F-FDG-avid osseous lesions in clinical practice, that, on review by a fellowship musculoskeletal trained radiologist, do not warrant biopsy because these lesions are classic "do not touch lesions" including non-ossifying fibromas, bone islands/enostoses, unicameral bone cysts, bone infarcts, and geodes/subchondral cysts)[16] or have a classic computed tomography (CT) imaging appearance including

fibrous dysplasia, Paget's disease and enchondromas. The "do not touch" osseous lesions are mostly benign osseous lesions; however, some may rarely undergo malignant degeneration. The term "do not touch" was coined by Clyde Helms, and refers to lesions that the radiographic/CT appearance is pathognomic, and additional diagnostic tests, biopsies and surgery involving these lesions may be misleading, potentially harming the patient[16]. Numerous case reports exist in the literature demonstrating that several of these benign lesions have resulted in $^{18}$F-FDG-avid osseous lesions and were confirmed histologically by subsequent biopsy[17-22].

While image-guided percutaneous core needle biopsy of osseous lesions is generally regarded as a low-risk procedure, potential complications exist, including patient discomfort and anxiety, infection, bleeding, and the possibility of a non-diagnostic specimen. Non-diagnostic biopsies may occur in 5-29% of cases and may lead to repeat percutaneous or subsequent open biopsy[23,24]. Although the CT imaging characteristics of an osseous lesion may indicate its non-aggressive etiology, clinicians may persistently request biopsies of $^{18}$F-FDG-avid osseous lesions in patients that have a primary malignancy elsewhere due to concerns of under-staging or clinical concerns centered around missing osseous metastases.

To date, despite multiple case reports of $^{18}$F-FDG-avid benign osseous lesions in the literature, to the best of our knowledge a descriptive analysis of the $^{18}$F-FDG uptake of common benign osseous lesions in the musculoskeletal system has not been performed. There are no prior reports demonstrating the spectrum of $^{18}$F-FDG uptake patterns of several common benign skeletal osseous lesions with identifiable CT imaging characteristics. If this data existed, then it could be used as a guide for physicians that primarily interpret $^{18}$F-FDG PET/CTs and to eliminate referral of these benign lesions for biopsies. The aim of the study is to show that "do not touch" and benign osseous lesions can have increased $^{18}$F-FDG uptake above blood-pool, therefore the CT appearance of these osseous lesions should dictate management rather than the PET/CT standardized uptake values (SUV).

## MATERIALS AND METHODS

### *Patient population*

This retrospective study included patients who had PET/CT imaging at our institution between January 1, 2006, and December 1, 2018. PET/CT studies were performed for staging or surveillance of malignancies or for the evaluation of a solitary pulmonary nodule. Lesions were identified by retrospective review of radiology text reports using Nuance mPower powered by Montage software (Burlington, MA) to identify potential PET/CT cases by searching for each of the following terms: "bone infarct"; "bone island"; "enchondroma"; "fibrous dysplasia"; "bone cyst or geode or herniation pit or subchondral cyst"; "myositis ossificans"; "osteochondroma"; "Paget's disease"; "hemangioma"; "non-ossifying fibroma"; "insufficiency fracture" and "osteomyelitis".

A sequential search was performed in which radiology text reports were searched first for the lesion of interest regardless of modality using the same search terms described above and then filtered by patients for which a PET/CT was available in the system within 3000 days prior to (excluding insufficiency fractures and infections) or following the study identifying the lesion. Lesions had to be stable in size and appearance for 2 years to confirm their non-aggressive nature. The imaging studies were each reviewed and the final lesion diagnosis was made/confirmed by a musculoskeletal radiologist with 6 years of experience and a musculoskeletal fellow in consensus. Imaging criteria used to classify each bone lesion will be discussed in detail in the discussion.

Non-ossifying fibromas (NOFs) were excluded because there were less than 5 patients with NOFs that had PET/CT imaging of the NOFs in our database, since NOFs typically occur in the extremities and were often excluded using the limited whole body (skull base to upper thigh)[25] field of view (FOV) and because most NOFs involute in early-adulthood.

Myositis ossificans was also excluded because analysis of the small number of cases identified by searching radiology reports.

### *PET/CT examination acquisition parameters*

Lesions were evaluated using one of the following PET/CT units: Philips Ingenuity TF PET/CT (Philips Medical Systems, Patient Port (Bore): 70 cm, Axial FOV: 18 cm, Detector Design: 4 × 4 × 22 mm LYSO crystals, Spatial Resolution: 4.7 mm full width at half maximum (FWHM); Philips Gemini TF small bore (Philips Medical Systems, Patient Port Bore: 70 cm, Reconstructed FOV: 25.6, 57.6, or 67.6 cm, Axial FOV: 18 cm,

Detector Design: 4 × 4 × 22 mm LYSO crystals, Spatial Resolution: 4.7 mm FWHM); or Phillips Gemini TF large bore (Philips Medical Systems, Patient Port Bore: 85 cm, Reconstructed FOV: 25.6, 57.6, or 67.6 cm, Axial FOV: 18 cm, Detector Design: 4 × 4 × 22 mm LYSO crystals, Spatial Resolution: 4.7 mm FWHM).

Patients underwent PET/CT examination according to institutional standard protocol, including fasting for 6 h prior to injection, followed by intravenous injection of 8-20 mCi (296-740 MBq) $^{18}$F-FDG, depending on body habitus. Blood glucose levels had to be less than 200 mg/dL (< 11.1 mmol/L) prior to injection. Approximately 225 mL of dilute barium oral contrast was administered before and thirty minutes after the administration of $^{18}$F-FDG if included in the imaging protocol. Images were acquired approximately 60 min (+/- 10 min) after the intravenous administration of $^{18}$F-FDG with the patient positioned supine on the scan table. Images were acquired from skull-base to thigh or from head to toe according to the imaging protocol, with low-dose CT images followed by PET images. Low-dose CT images were obtained with a slice thickness of 4 mm, pitch of 0.8, tube voltage of 120 kVp, and tube current of 70 mAs.

### *SUV measurements*

SUV measurements were obtained using MIM (version 6.7.10, Mim Software Inc.). A region of interest was drawn around each lesion using the SUV tool and the maximum and mean SUV recorded. Subsequently, the mean and max SUV were also measured for the liver, and for the blood pool, which was measured in the mediastinum at the level of the aorta and main pulmonary artery. The mean (standard deviation) and maximum SUV for each lesion was measured and reported both independently and in relation to the mean blood pool SUV on the examination, measured at the level of the great vessels in the mediastinum, to correct for slight variations in technique that affect SUV measurement [26].

### *Statistics*

Descriptive statistics were calculated using R v3.5 (https://www.r-project.org/). Pearson's correlations between the size of lesions and the maximum SUV were calculated.

### *Research ethics standards compliance*

This retrospective Health Insurance Portability and Accountability Act (HIPAA) compliant study was approved by the local institutional review board (IRB) (Protocol Number: 828078, Confirmation #: Cefchdfh), and the need for signed informed consent was waived.

## RESULTS

There were 287 patients with either classic "do not touch" lesions or classic benign lesions. Patient characteristics are summarized in Table 1. Figure 1 shows the $^{18}$F-FDG avidity of each lesion type. Benign cystic lesions included subchondral cysts, bone cysts, herniation pits, and geodes. The maximum SUV detected was lowest for osteochondromas (maximum SUV 2.56), enchondromas (maximum SUV 2.69), and hemangiomas (maximum SUV of 2.88). The maximum SUV was highest for Paget's disease of bone (maximum SUV of 5.65), benign cystic lesions (maximum SUV of 6.5), osteomyelitis (maximum SUV of 12.64), insufficiency fractures (maximum SUV of 12.97), and fibrous dysplasia (maximum SUV of 18.63) (Table 2). There was at least one lesion amongst each lesion type evaluated that demonstrated greater $^{18}$F-FDG avidity than the blood pool, with the highest maximum SUV ranging from 9.34 times blood pool mean (osteomyelitis) to 1.42 times blood pool mean (hemangioma) (Table 2, Figure 1A and 1B).

There was no correlation between the maximum SUV and the size of benign cystic lesions ($r$ = 0.08, $P$ = 0.60), hemangiomas ($r$ = 0.15, $P$ = 0.44), bone infarcts ($r$ = 0.12, $P$ = 0.37), fibrous dysplasia ($r$ = 0.13, $P$ = 0.48), osteochondromas ($r$ = 0.04, $P$ = 0.95), Paget's disease of bone ($r$ = 0.16, $P$ = 0.50), insufficiency fractures ($r$ = 0.01, $P$ = 0.96) and osteomyelitis ($r$ = 0.15, $P$ = 0.60). However, the size of enchondromas was associated with the maximum SUV ($r$ = 0.36, $P$ = 0.02).

## DISCUSSION

The "do not touch" and benign lesions evaluated demonstrated a range of SUV values. All evaluated "do not touch" and benign lesions had at least one lesion with

**Table 1 Patient characteristics by lesion type**

| Lesion type | Mean patient age (yr) | Range patient age (yr) | Male (%) |
|---|---|---|---|
| Benign cystic lesions ($n$ = 42) | 63.2 | 36-92 | 69.0 |
| Hemangioma ($n$ = 29) | 68.5 | 47-88 | 55.2 |
| Bone infarct ($n$ = 16) | 58.7 | 33-74 | 62.5 |
| Bone island ($n$ = 56) | 63.0 | 37-90 | 50.0 |
| Enchondroma ($n$ = 45) | 64.6 | 52-84 | 46.7% |
| Fibrous dysplasia ($n$ = 26) | 56.1 | 28-86 | 76.9 |
| Osteochondroma ($n$ = 6) | 61.3 | 43-80 | 100.0 |
| Paget's disease of bone ($n$ = 20) | 73.4 | 59-86 | 80.0 |
| Insufficiency fracture ($n$ = 32) | 69.1 | 47-89 | 6.3 |
| Osteomyelitis ($n$ = 15) | 62.8 | 32-83 | 73.3 |

Benign cystic lesions: Subchondral cysts, bone cysts, herniation pits, and geodes.

maximum SUV that was greater than and at least one lesion with maximum SUV that was less than the mean blood pool SUV. For this reason, the results suggest that the maximum SUV is not a reliable tool for the characterization of osseous lesions, particularly as benign lesions such as fibrous dysplasia can demonstrate a maximum SUV up to 8.87 times the average blood pool SUV.

These findings are consistent with multiple case reports in the literature that have described pathology-proven benign lesions with high $^{18}$F-FDG avidity prompting surgical excision on the basis of the $^{18}$F-FDG uptake[7,17-22]. Our results reaffirm that, when specific, the CT characteristics of such lesions need not be accompanied by an SUV at or below that of the blood pool to confidently diagnose a lesion as benign. In fact, SUV values may be misleading, and over-reliance on $^{18}$F-FDG uptake to characterize a lesion as benign or malignant may lead to over-diagnosis and unnecessary procedures such as biopsies, which although low-risk, are not risk-free.

Benign cystic lesions, including bone cysts, geodes, and herniation pits, have in common a well circumscribed, lytic appearance [27-30]. All may have a sclerotic rim, although such a rim is only occasionally present in simple bone cysts [27]. The terms geode and herniation pit both describe lesions arising in the setting of reactive changes at the surface of bone, although herniation pits have classically been described in the femoral neck, remote from the articular surface, whereas geodes are subarticular in location and regarded as synonymous with subchondral cysts (Figure 2), although these lesions lack an epithelial lining and are not true cysts[31]. Subchondral cysts/geodes are often accompanied by other signs of joint degeneration including subchondral sclerosis and eburnation as well as marginal osteophyte formation. Subchondral cysts are more common in the elderly. These lesions are lytic on CT and may show increased $^{18}$F-FDG uptake on PET.

Osseous hemangiomas are most commonly seen in the vertebral bodies, but may occur in the calvarium, calcaneus, and long bones [28]. Vertebral body hemangiomas have a characteristic striated appearance on radiographs and a corresponding "polka dot" appearance on axial CT images (Figure 3A)[28]. On MRI, hemangiomas typically have high signal on both T1- and T2-weighted images[32] and commonly show loss of signal on in- and out-of-phase gradient sequences[33]. The PET/CT appearance is similar to the CT appearance, with some lesions showing increased $^{18}$F-FDG uptake on PET.

The term "bone infarct" is commonly used to refer to osteonecrosis seen in the metaphyses and diaphyses of bones [34], whereas osteonecrosis occurring in the epiphysis is commonly referred to as avascular necrosis. On CT, these lesions may demonstrate a serpentine rim of sclerosis (Figure 3B), although this may not be seen early in the disease course [32]. Bone infarcts have a similar appearance on PET/CT to CT, but may show variable amounts of $^{18}$F-FDG uptake on PET. On MRI, these lesions demonstrate a characteristic serpentine rim of low signal with variable internal signal [34]. Bone infarcts rarely undergo malignant degeneration, most commonly into osteosarcoma, pleomorphic sarcoma and fibrosarcoma, but here malignant degeneration is characterized by development of a soft tissue mass, cortical destruction and in some cases development of a pathological fracture [35].

Bone islands, or enostoses, are benign osteoblastic lesions consisting of dense intramedullary lamellar bone that appear on CT as hyperdense oval lesions with spiculated margins and are classically periarticular (Figure 4A)[28]. The data presented

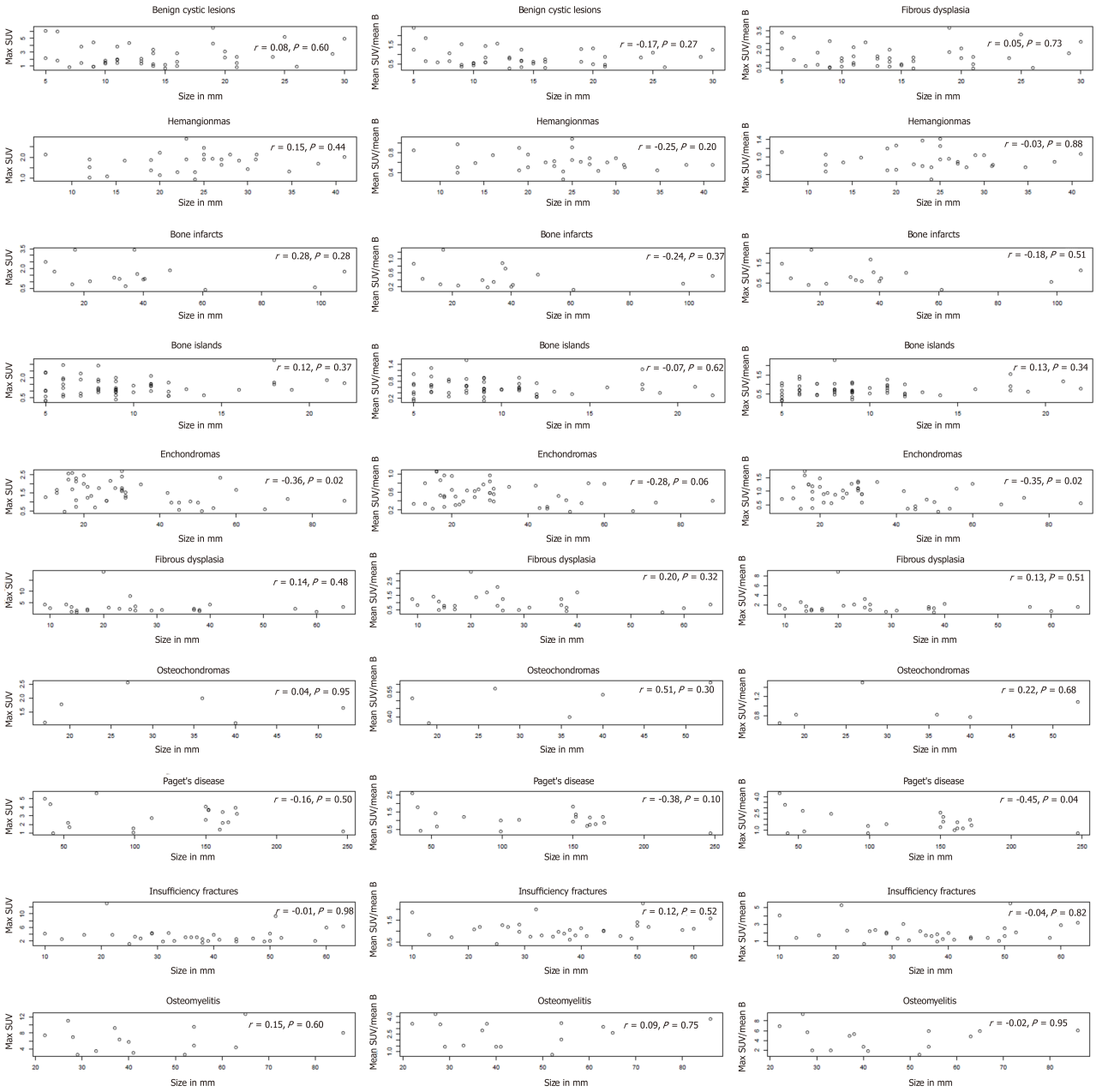


**Figure 1 Plots of maximum standardized uptake value values, mean standardized uptake value/mean blood pool, and maximum standardized uptake value/blood pool by lesion size for each lesion type.** SUV: Standardized uptake value; Max SUV: Maximum standardized uptake value; Mean SUV/Mean B: Mean standardized uptake value divided by the mean blood pool uptake; Max SUV/Mean B: Maximum standardized uptake value divided by the mean blood pool uptake.

show that enostoses appear similar on PET/CT to CT and may show $^{18}$F-FDG uptake on PET above background. Although osteoblastic metastatic lesions may have a similar appearance, bone islands can be identified with high sensitivity and specificity by their higher attenuation value on CT[36]. On MRI, osteoblastic metastases may also show a halo of surrounding bone marrow edema, which may help distinguish these lesions from bone islands[28].

Enchondromas are benign lesions that typically occur within long bones. Enchondromas histologically represent rests of hyaline cartilage within medullary bone. Radiographically, enchondromas are expansile lucent lesions with a narrow zone of transition and varying degrees of ring-and-arc mineralization (Figure 4B)[28], although mineralization may be absent when these lesions are seen in the hands and feet. Enchondromas are almost never seen involving the flat bones (ribs, pelvis, scapula) or spine. Distinguishing between enchondromas and chondrosarcomas can be challenging, both by imaging features and by histology[37]. Malignant degeneration may be seen and is more common (20%-50%) in patients with Ollier disease or Maffucci syndrome[28]. Malignant degeneration is characterized by increase in size of lesion after skeletal maturity and pain[37,38]. A prior report suggested that a maximum

**Table 2 18-F-fluorodeoxyglucose positron emission tomography/computed tomography standardized uptake value by lesion type**

| Lesion type | Range of the max SUV | Median (interquartile range) of the max SUV | Mean SUV (SD) | Proportion with max SUV > 3.0 (%) | Maximum SUV/mean blood Pool SUV range | Maximum SUV /mean blood pool SUV median (interquartile range) | Proportion of lesions with maximum SUV > mean blood pool (maximum SUV/mean blood pool SUV > 1.0) (%) |
|---|---|---|---|---|---|---|---|
| Benign cystic lesions (*n* = 42) | 0.68-6.5 | 1.90 (1.34-3.27) | 1.38 (0.86) | 28.6 | 0.5-3.74 | 1.29 (0.76-1.94) | 64.3 |
| Hemangioma (*n* = 29) | 0.95-2.88 | 1.86 (1.38-2.00) | 1.14 (0.30) | 0 | 0.49-1.42 | 0.88 (0.78-1.05) | 34.5 |
| Bone infarct (*n* = 16) | 0.37-3.44 | 1.27 (0.95-1.80) | 0.80 (0.54) | 12.5 | 0.15-2.18 | 0.75 (0.57-1.08) | 37.5 |
| Bone island (*n* = 56) | 0.26-3.29 | 1.18 (0.91-1.73) | 1.04 (0.52) | 1.8 | 0.13-2.28 | 0.69 (0.53-0.98) | 25.0 |
| Enchondroma (*n* = 45) | 0.46-2.69 | 1.49 (1.05-1.98) | 0.93 (0.43) | 0.0 | 0.25-1.72 | 0.90 (0.58-1.15) | 42.2 |
| Fibrous dysplasia (*n* = 26) | 0.78-18.63 | 2.07 (1.56-3.04) | 1.80 (1.40) | 30.8 | 0.49-8.87 | 1.35 (0.89-1.93) | 69.2 |
| Osteochondroma (*n* = 6) | 1.11-2.56 | 1.71 (1.25-1.93) | 0.89 (0.09) | 0 | 0.64-1.50 | 0.82 (0.78-1.02) | 33.3 |
| Paget's disease of bone (*n* = 20) | 0.93-5.65 | 2.59 (1.66-3.79) | 1.77 (0.82) | 45.0 | 0.70-4.30 | 1.45 (1.10-2.23) | 75.0 |
| Insufficiency fracture (*n* = 32) | 1.06-12.97 | 2.95 (2.05-4.09) | 1.82 (0.68) | 46.9 | 0.64-5.43 | 1.76 (1.33-2.25) | 90.6 |
| Osteomyelitis (*n* = 15) | 2.57-12.64 | 6.40 (3.99-8.63) | 3.77 (1.31) | 80.0 | 1.07-9.34 | 4.88 (2.34-5.88) | 100 |

Benign cystic lesions: Subchondral cysts, bone cysts, herniation pits, and geodes. SUV: Standardized uptake value.

SUV > 4.4 was 99% specific for grade 2/3 chondrosarcoma[39]. Biopsy of low-grade chondroid matrix lesions, such as enchondromas, is of limited utility because enchondromas may be histologically mistaken for low-grade chondrosarcomas and vice versa. Enchondromas have a similar appearance on PET/CT to CT and radiographs, but may show variable amounts of $^{18}$F-FDG uptake on PET. The data suggest that the size of the enchondroma is associated with higher maximum SUV; however, it is unclear whether this confers a potentially higher risk for chondrosarcoma. Development of a soft tissue mass with cortical destruction is highly suspicious for malignant degeneration.

Fibrous dysplasia is due to a post-natal sporadic mutation in the G-nucleotide binding protein alpha sub unit (GNAS) and results in development of fibrous tissue with ground-glass matrix on radiographs and CT studies[40]. Fibrous dysplasia may have areas of cystic change on CT. The PET/CT appearance of fibrous dysplasia is identical to its appearance on CT; however, fibrous dysplasia may be metabolically active and show increased $^{18}$F-FDG uptake. Fibrous dysplasia may be monostotic or polyostotic. McCune-Albright syndrome is associated with polyostotic fibrous dysplasia, café au lait macules and hyperfunctioning endocrinopathies, which may include precocious puberty, hyperthyroidism or Cushing's syndrome. Mazabraud syndrome is characterized by fibrous dysplasia with intramuscular myxomas. Fibrous dysplasia typically affects ribs and long bones (femur, tibia, and humerus), and may result in a Shepherd's crook deformity of the femurs. Fibrous dysplasia may involve the bones of the face/jaw and result in disfigurement, or involve the spine and result in scoliosis. Approximately 1% of patients will have a lesion that undergoes malignant degeneration, most commonly into osteosarcoma, fibrosarcoma or undifferentiated pleomorphic sarcoma[40,41]. Malignant degeneration is characterized by development of an osteolytic component with cortical destruction[41].

Osteochondromas are tumors of the bone that may be sporadic or inherited. These are bony exostoses that show contiguity with the intramedullary canal on CT studies (Figure 5A). These exostoses have a cartilage cap that may be along various stages of ossification. Osteochondromas should not grow after skeletal maturity. Osteochondromas may be sessile or pedunculated, and if pedunculated point away from

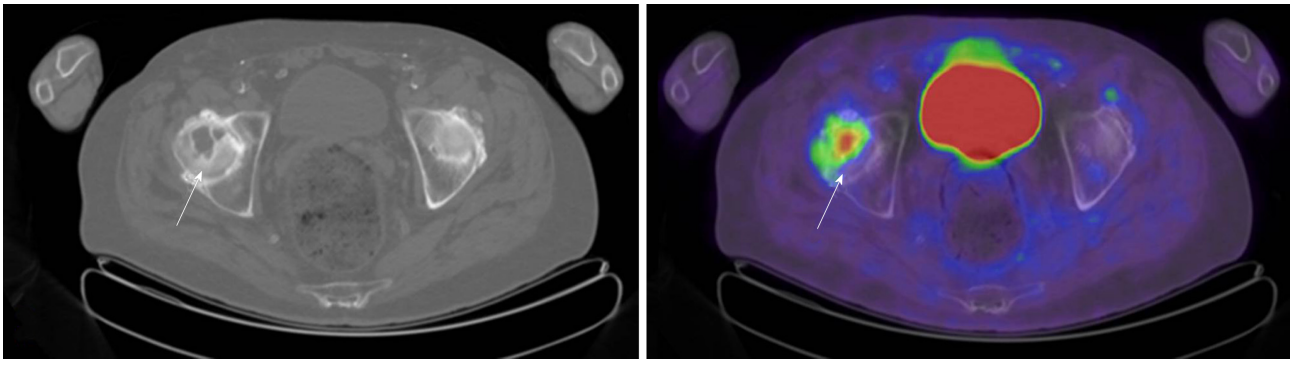

**Figure 2 Axial computed tomography and axial fused positron emission tomography/computed tomography of the pelvis in an 82-year-old male with history of colon and parotid gland cancer with subchondral cyst in the right femoral head (arrows) (maximum standardized uptake value 5.2).**

the nearest joint. Osteochondromas are benign tumors, but may rarely undergo malignant degeneration into a chondrosarcoma. Malignant degeneration is more common in patients with multiple hereditary exostoses (MHE). A thickened cartilage cap on CT, greater than 2.0 cm, has been reported as 100% sensitive and 95% specific for degeneration into chondrosarcoma[42]. The communication of the bony excrescence with the intramedullary space on PET/CT is pathognomic; however, osteochondromas should not be confused with tubercles/muscle insertion sites. Osteochondromas may show increased $^{18}$F-FDG uptake on PET/CT.

Paget's disease of the bone is a disorder of normal bone homeostasis with abnormal osteoblastic and osteoclastic activity. The exact etiology of Paget's disease is unknown; however, Paget's disease may present in a mixture of three phases: the osteolytic phase, the intermediate phase, and the quiescent phase. Pagetic bone in osteolytic phase may show osteolytic lesions, like osteoporosis circumscripta cranii; however, Pagetic bone in the intermediate and quiescent phase shows cortical and trabecular thickening on CT (Figure 5B). The PET/CT appearance of Paget's disease is identical to that noted on CT; however, Paget's disease may show variable $^{18}$F-FDG uptake, likely depending on the phase of Paget's disease. A proximal femur shepherd's crook deformity may be present. Paget's disease tends to be localized affecting adjacent bones. The cotton wool spots/patchy areas of sclerosis of Paget's disease are often mistaken for osteoblastic metastases, in particular metastases related to prostate or breast cancer. While Paget's disease is benign, Pagetic bone may rarely undergo malignant degeneration into undifferentiated pleomorphic sarcoma, fibrosarcoma, or osteosarcoma amongst other sarcomas[43]. Development of a soft tissue mass with cortical destruction should be considered highly suspicious for malignant degeneration of Paget's disease.

Insufficiency fractures can occur in patients after radiation, after chemotherapy, or after hormonal-altering therapy for some cancers including breast and prostate cancer, or be related to diminished bone mineral density related to senescent changes. Insufficiency fractures are more common in women. Acute sacral insufficiency fractures appear as unilateral or bilateral para-median linear lucencies with adjacent sclerosis oriented anterior-posterior along the sacral ala on CT (Figure 6A); however, a transverse component may be present, resulting in a "Honda" or "H" sign on Tc99m-MDP bone scans and PET/CT. Insufficiency fractures may also be noted involving the iliac wing, medial ilium, supraacetabular region, parasymphyseal region, and involving the pubic rami[44]. Proximal femoral insufficiency fractures are more common along the compression than tension side of the hip; however, insufficiency fractures related to bisphosphonate therapy are more common along the tension side of the sub-trochanteric proximal femur.

Osteomyelitis is an infection of the intramedullary canal and cortex of the bone. Signs of osteomyelitis may include elevated white blood cell counts (WBC), erythrocyte sedimentation rate (ESR) and C-reactive protein (CRP). Clinical history and physical examination are often required because the yield for bone biopsies for osteomyelitis is generally less than 50%. CT findings of osteomyelitis include periosteal reaction, sclerosis, osseous erosion/destruction, surrounding soft tissue inflammatory changes and reactive lymphadenopathy (Figure 6B). These areas of destruction may show increased $^{18}$F-FDG uptake depending on chronicity on PET/CT. Longstanding chronic ulcers (Marjolin's ulcers) related to chronic infection, burns, injuries, or venous stasis and chronic osteomyelitis may undergo malignant degeneration into squamous cell or basal cell carcinoma [44,45]. Signs of malignant degeneration include development of bone destruction, soft tissue mass and per-

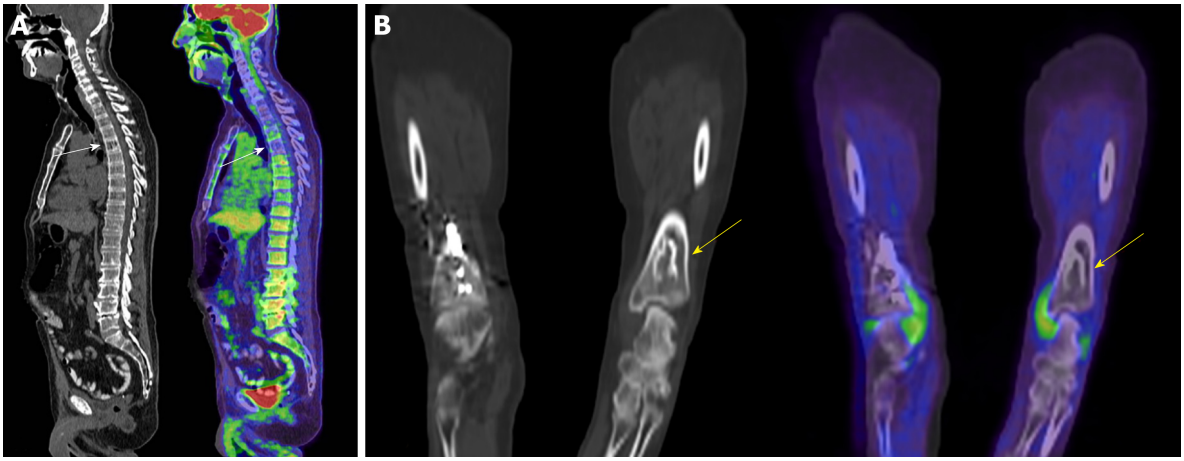


**Figure 3 Computed tomography and fused positron emission tomography/computed tomography of two patients.** A: Sagittal computed tomography (CT) and sagittal fused positron emission tomography (PET)/CT of the spine in a 73-year-old male with history of lymphoma and a hemangioma in the T5 vertebral body (arrows) [maximum standardized uptake value (SUV) 2.86]; B: Coronal CT and coronal fused PET/CT of the distal tibia in a 54-year-old female with history of a neuroendocrine lung tumor demonstrating a bone infarct (arrows) in the distal tibia (maximum SUV 0.37).

iosteal reaction[44,45].

These findings are clinically important for radiologists and clinicians, because we have described the key CT imaging features of these "do not touch" and benign lesions, which can be gleaned from the CT component of the PET/CT. We anticipate that this will decrease the number of times the PET/CT interpreting physician and the bone biopsy proceduralist have differing opinions and reduce the number of unnecessary bone biopsies.

This study has a few limitations. The data are obtained from a single center tertiary care academic healthcare center, and therefore subject to ascertainment bias since our institution primarily treats adult patients. Lesions that are more common in the pediatric population including cortical desmoids and avulsion fractures were not described. SUV measurements, while standardized by weight, acquisition time, and injected dose, may be affected by body mass index, scanner calibration, and imaging artifacts, among other factors[26]. To address this limitation, blood pool mean SUV was included as an internal control to better characterize the FDG uptake of the target lesions. Several lesions were not histologically confirmed – this was because these lesions had the classic imaging appearance of a benign lesion or a "do not touch" lesion[16], and biopsies of these lesions are generally thought to be unnecessary since characterization by a trained musculoskeletal radiologist is pathognomic. The sample size was limited, but these are rare lesions, and prior publications referencing these lesions are almost all are restricted to case-reports. Nonetheless, this work clearly shows the spectrum of $^{18}$F-FDG uptake in several known "do not touch" and benign osseous lesions, which can be used to help in clinical decision making.

In conclusion, among benign lesions for which CT imaging findings are diagnostic, SUV values may vary, and these lesions may demonstrate $^{18}$F-FDG uptake above that of the blood pool. For this reason, $^{18}$F-FDG uptake above background should not be misconstrued to indicate the presence of malignancy for all osseous lesions.

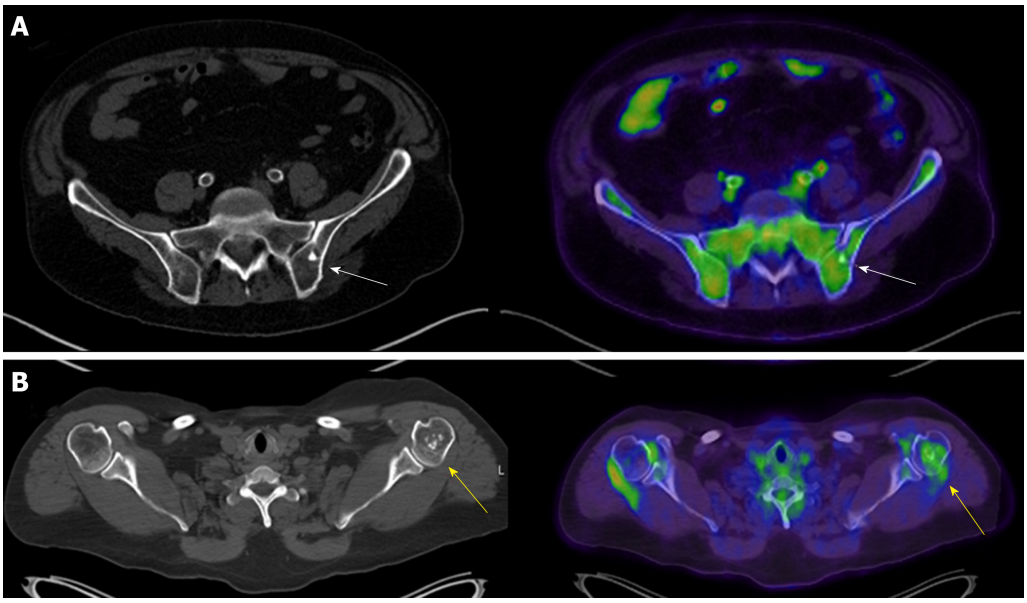


**Figure 4 Axial computed tomography and axial fused positron emission tomography/computed tomography of two patients.** A: Axial computed tomography (CT) and axial fused positron emission tomography (PET)/CT of the pelvis in a 76-year-old male with a history of a solitary pulmonary nodule and a bone island in his left ilium (arrows); B: Axial CT and axial fused PET/CT of the chest in a 52-year-old female with a history of melanoma and an enchondroma in the left proximal humerus (arrows) (maximum standardized uptake value 2.33).

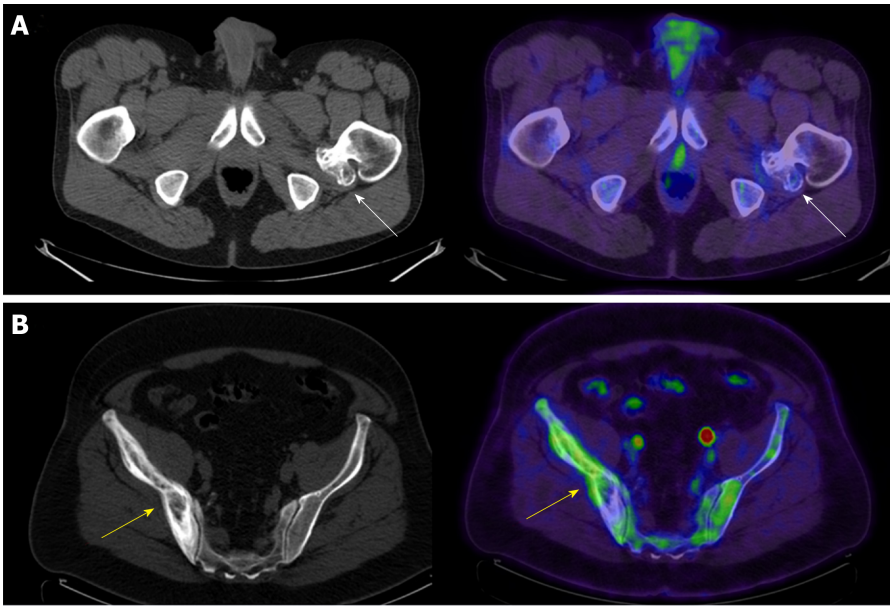


**Figure 5 Axial computed tomography and axial fused positron emission tomography/computed tomography of two patients.** A: Axial computed tomography (CT) and axial fused positron emission tomography (PET)/CT of the pelvis in a 51-year-old male with diffuse large B-cell lymphoma and a sessile osteochondroma arising from the proximal left femur (arrows) [maximum standardized uptake value (SUV) 1.64]; B: Axial CT and axial fused PET/CT of the pelvis in a 61-year-old male with a history of a follicular lymphoma and Paget's disease of the bone involving the right ilium (arrows) (maximum SUV 3.92).

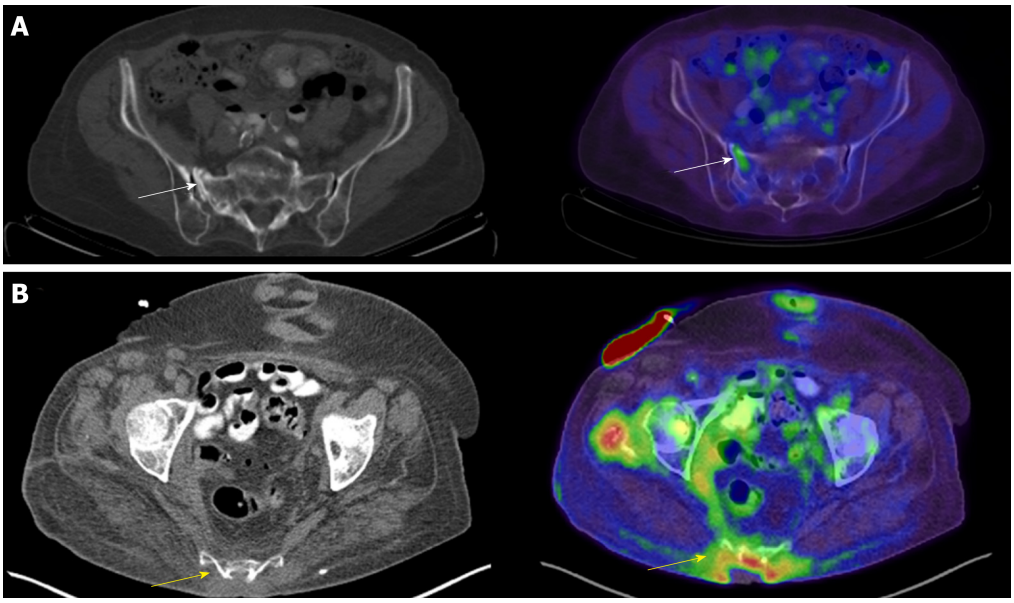


**Figure 6 Axial computed tomography and axial fused positron emission tomography/computed tomography of two patients.** A: Axial computed tomography (CT) and axial fused positron emission tomography (PET)/CT of the pelvis in an 84-year-old female with a history of non-Hodgkin's lymphoma and an insufficiency fracture of the right sacral ala (arrows) [maximum standardized uptake value (SUV) 1.99]; B: Axial CT and axial fused PET/CT of the pelvis in an 82-year-old female with a sacral decubitus ulcer and osteomyelitis (arrows).

## ARTICLE HIGHLIGHTS

### *Research background*

18-F-fluorodeoxyglucose ($^{18}$F-FDG) positron emission tomography/computed tomography (PET/CT) is increasingly used for staging and monitoring of many common malignancies. Classical "do not touch" and benign bone lesions are sometimes detected in $^{18}$F-FDG PET/CT studies. These lesions may be referred for biopsy because the PET/CT interpreting physician may be unfamiliar with the spectrum of the $^{18}$F-FDG PET/CT uptake pattern exhibited by these lesions.

### *Research motivation*

There is no descriptive analysis of $^{18}$F-FDG uptake of "do not touch" and benign osseous lesions.

### *Research objectives*

This study evaluates the spectrum of $^{18}$F-FDG PET/CT uptake patterns in several "do not touch" and benign osseous lesions to provide a reference for physicians interpreting $^{18}$F-FDG PET/CTs .

### *Research methods*

This study evaluated 287 independent patients, of whom 287 were classic "do not touch" (benign cystic lesions, insufficiency fractures, bone islands, bone infarcts) or benign osseous lesions (hemangiomas, enchondromas, osteochondromas, fibrous dysplasia, Paget's disease, osteomyelitis) $^{18}$F-FDG PET/CT from January 1, 2006 to December 1, 2018 at a single academic institution. The maximum and mean standardized uptake values (SUV), and the ratio of the maximum SUV to mean blood pool were calculated. Pearson's correlations between lesion size and maximum SUV were calculated.

### *Research results*

The maximum SUV range was as follows: hemangiomas (0.95-2.99), bone infarcts (0.37-3.44), bone islands (0.26-3.29), enchondromas (0.46-2.69), fibrous dysplasia (0.78-18.63), osteochondromas (1.11-2.56), Paget's disease of bone (0.93-5.65), insufficiency fractures (1.06-12.97) and for osteomyelitis (2.57-12.64). The upper range of the maximum SUV was lowest for Osteochondromas (maximum SUV 2.56). The upper range of the maximum SUV was highest for fibrous dysplasia (maximum SUV of 18.63). In each lesion type, at least one lesion showed greater $^{18}$F-FDG activity than the blood pool, with the highest maximum SUV up to 9.34 times the blood pool average (osteomyelitis) to the blood pool average (hemangioma) 1.42 times. Except for enchondromas, there was no correlation between the maximum SUV and the size of the lesion. Larger enchondromas have a higher maximum SUV ($r$ = 0.36, $P$ = 0.02).

### *Research conclusions*

"Do not touch" and benign osseous lesions may exhibit $^{18}$F-FDG uptake higher than in the blood pool on PET/CT. Therefore, $^{18}$F-FDG uptake above blood pool should not be misunderstood to indicate the presence of malignancy. The CT appearance, if pathognomic should be used to guide management rather than the maximum SUV.

### *Research perspectives*

The data comes from an academic tertiary health care center that primarily treats adult patients. More common lesions in the pediatric population, including cortical desmoids and avulsion fractures, were not described. Although SUV measurements were normalized by weight, acquisition time and injection dose, they may be affected by factors such as body mass index, scanner calibration and imaging artifacts.

## REFERENCES


1 **Valk PE**, Pounds TR, Tesar RD, Hopkins DM, Haseman MK. Cost-effectiveness of PET imaging in clinical oncology. *Nucl Med Biol* 1996; **23**: 737-743 [PMID: 8940715 DOI: 10.1016/0969-8051(96)00080-7]

2 **Hicks RJ**. Should positron emission tomography/computed tomography be the first rather than the last test performed in the assessment of cancer? *Cancer Imaging* 2012; **12**: 315-323 [PMID: 23022990 DOI: 10.1102/1470-7330.2012.9005]

3 Available from: https://imvinfo.com/product/pet-imaging-market-summary-report-2018/

4 **Czernin J**, Allen-Auerbach M, Nathanson D, Herrmann K. PET/CT in Oncology: Current Status and Perspectives. *Curr Radiol Rep* 2013; **1**: 177-190 [PMID: 24883234 DOI: 10.1007/s40134-013-0016-x]

5 **Warburg O**, Posener K, Negelein E. The metabolism of cancer cells. *Biochem Zeitschr* 1924; **152**: 129–169

6 **Warburg O**, Wind F, Negelein E. The metabolism of tumors in the body. *J Gen Physiol* 1927; **8**: 519-530 [PMID: 19872213 DOI: 10.1085/jgp.8.6.519]

7 **Wang G**, Lau EW, Shakher R, Rischin D, Ware RE, Hong E, Binns DS, Hogg A, Drummond E, Hicks RJ. How do oncologists deal with incidental abnormalities on whole-body fluorine-18 fluorodeoxyglucose PET/CT? *Cancer* 2007; **109**: 117-124 [PMID: 17133406 DOI: 10.1002/cncr.22370]

8 **Beatty JS**, Williams HT, Aldridge BA, Hughes MP, Vasudeva VS, Gucwa AL, David GS, Lind DS, Kruse EJ, McLoughlin JM. Incidental PET/CT findings in the cancer patient: how should they be managed? *Surgery* 2009; **146**: 274-281 [PMID: 19628085 DOI: 10.1016/j.surg.2009.04.024]

9 **Sebro R**, Aparici CM, Pampaloni MH. Frequency and clinical implications of incidental new primary cancers detected on true whole-body 18F-FDG PET/CT studies. *Nucl Med Commun* 2013; **34**: 333-339 [PMID: 23407371 DOI: 10.1097/MNM.0b013e32835f163f]

10 **European Society of Radiology 2009**. The future role of radiology in healthcare. *Insights Imaging* 2010; **1**: 2-11 [PMID: 22347897 DOI: 10.1007/s13244-009-0007-x]

11 **Mohan C**. Subspecialization in radiology - Is it time to hatch out of the cocoon? *Indian J Radiol Imaging* 2017; **27**: 261-262 [PMID: 29089669 DOI: 10.4103/ijri.IJRI_345_17]

12 **Thrall JH**, Wittenberg J. Radiology summit 1990: specialization in radiology--trends, implications, and recommendations. *AJR Am J Roentgenol* 1991; **156**: 1273-1276 [PMID: 2028877 DOI: 10.2214/ajr.156.6.2028877]

13 **Bluth EI**, Truong H, Nsiah E, Hughes D, Short BW. The 2013 ACR Commission on Human Resources workforce survey. *J Am Coll Radiol* 2013; **10**: 750-756 [PMID: 24091045 DOI: 10.1016/j.jacr.2013.06.010]

14 **Atlas SW**. Embracing subspecialization: the key to the survival of radiology. *J Am Coll Radiol* 2007; **4**: 752-753 [PMID: 17964496 DOI: 10.1016/j.jacr.2007.04.003]

15 **Pencharz D**, Nathan M, Wagner TL. Evidence-based management of incidental focal uptake of fluorodeoxyglucose on PET-CT. *Br J Radiol* 2018; **91**: 20170774 [PMID: 29243502 DOI: 10.1259/bjr.20170774]

16 **Brant WE**, Helms C. Fundamentals of Diagnostic Radiology. Lippincott Williams and Wilkins. 2012

17 **Döbert N**, Menzel C, Ludwig R, Berner U, Diehl M, Hamscho N, Grünwald F. Enchondroma: a benign osseous lesion with high F-18 FDG uptake. *Clin Nucl Med* 2002; **27**: 695-697 [PMID: 12352108 DOI: 10.1097/00003072-200210000-00001]

18 **Nakayama M**, Okizaki A, Ishitoya S, Aburano T. "Hot" vertebra on (18)F-FDG PET scan: a case of vertebral hemangioma. *Clin Nucl Med* 2012; **37**: 1190-1193 [PMID: 23154481 DOI: 10.1097/RLU.0b013e3182708628]

19 **Tripathi M**, Kumar R, Mohapatra T, Nadig M, Bal C, Malhotra A. Intense F-18 FDG uptake noted in a benign bone cyst. *Clin Nucl Med* 2007; **32**: 255-257 [PMID: 17314616 DOI: 10.1097/01.rlu.0000255272.96243.06]

20 **Charest M**, Singnurkar A, Hickeson M, Novales JA, Derbekyan V. Intensity of FDG uptake is not everything: synchronous liposarcoma and fibrous dysplasia in the same patient on FDG PET-CT imaging. *Clin Nucl Med* 2008; **33**: 455-458 [PMID: 18580228 DOI: 10.1097/RLU.0b013e31817793bb]

21 **Strobel K**, Merwald M, Huellner M, Zenklusen HR, Kuttenberger J. Osteoblastoma of the mandible mimicking osteosarcoma in FDG PET/CT imaging. *Clin Nucl Med* 2013; **38**: 143-144 [PMID: 23334133 DOI: 10.1097/RLU.0b013e318279f131]

22 **Mahmood S**, Martinez de Llano SR. Paget disease of the humerus mimicking metastatic disease in a patient with metastatic malignant mesothelioma on whole body F-18 FDG PET/CT. *Clin Nucl Med* 2008; **33**: 510-512 [PMID: 18580246 DOI: 10.1097/RLU.0b013e318177928a]

23 **Li J**, Weissberg Z, Bevilacqua TA, Yu G, Weber K, Sebro R. Concordance between fine-needle aspiration and core biopsies for osseous lesions by lesion imaging appearance and CT attenuation. *Radiol Med* 2018; **123**: 254-259 [PMID: 29249078 DOI: 10.1007/s11547-017-0841-8]

24 **Yang J**, Frassica FJ, Fayad L, Clark DP, Weber KL. Analysis of nondiagnostic results after image-guided needle biopsies of musculoskeletal lesions. *Clin Orthop Relat Res* 2010; **468**: 3103-3111 [PMID: 20383617 DOI: 10.1007/s11999-010-1337-1]

25 **Sebro R**, Mari-Aparici C, Hernandez-Pampaloni M. Value of true whole-body FDG-PET/CT scanning protocol in oncology: optimization of its use based on primary diagnosis. *Acta Radiol* 2013; **54**: 534-539 [PMID: 23463863 DOI: 10.1177/0284185113476021]

26 **Adams MC**, Turkington TG, Wilson JM, Wong TZ. A systematic review of the factors affecting accuracy of SUV measurements. *AJR Am J Roentgenol* 2010; **195**: 310-320 [PMID: 20651185 DOI: 10.2214/AJR.10.4923]

27 **Parman LM**, Murphey MD. Alphabet soup: cystic lesions of bone. *Semin Musculoskelet Radiol* 2000; **4**:

89-101 [PMID: 11061694 DOI: 10.1055/s-2000-6857]
28 **Motamedi K**, Seeger LL. Benign bone tumors. *Radiol Clin North Am* 2011; **49**: 1115-1134, v [PMID: 22024291 DOI: 10.1016/j.rcl.2011.07.002]
29 **Pitt MJ**, Graham AR, Shipman JH, Birkby W. Herniation pit of the femoral neck. *AJR Am J Roentgenol* 1982; **138**: 1115-1121 [PMID: 6979213 DOI: 10.2214/ajr.138.6.1115]
30 **Resnick D**, Niwayama G, Coutts RD. Subchondral cysts (geodes) in arthritic disorders: pathologic and radiographic appearance of the hip joint. *AJR Am J Roentgenol* 1977; **128**: 799-806 [PMID: 404905 DOI: 10.2214/ajr.128.5.799]
31 **Resnick D**. *Bone and Joint Imaging, 2nd ed*. Philadelphia, PA: WB Saunders Company; 1996; 325-327
32 **Kwee TC**, de Klerk JMH, Nix M, Heggelman BGF, Dubois SV, Adams HJA. Benign Bone Conditions That May Be FDG-avid and Mimic Malignancy. *Semin Nucl Med* 2017; **47**: 322-351 [PMID: 28583274 DOI: 10.1053/j.semnuclmed.2017.02.004]
33 **Perry MT**, Sebro R. Accuracy of Opposed-phase Magnetic Resonance Imaging for the Evaluation of Treated and Untreated Spinal Metastases. *Acad Radiol* 2018; **25**: 877-882 [PMID: 29398437 DOI: 10.1016/j.acra.2017.11.022]
34 **Hara H**, Akisue T, Fujimoto T, Kishimoto K, Imabori M, Kishimoto S, Kawamoto T, Yamamoto T, Kuroda R, Fujioka H, Doita M, Kurosaka M. Magnetic resonance imaging of medullary bone infarction in the early stage. *Clin Imaging* 2008; **32**: 147-151 [PMID: 18313581 DOI: 10.1016/j.clinimag.2007.07.005]
35 **McDonald MD**, Sadigh S, Weber KL, Sebro R. A Rare Case of an Osteolytic Bone-infarct-associated Osteosarcoma: Case Report with Radiographic and Histopathologic Correlation, and Literature Review. *Cureus* 2018; **10**: e2777 [PMID: 30112253 DOI: 10.7759/cureus.2777]
36 **Elangovan SM**, Sebro R. Accuracy of CT Attenuation Measurement for Differentiating Treated Osteoblastic Metastases From Enostoses. *AJR Am J Roentgenol* 2018; **210**: 615-620 [PMID: 29323547 DOI: 10.2214/AJR.17.18638]
37 **Murphey MD**, Flemming DJ, Boyea SR, Bojescul JA, Sweet DE, Temple HT. Enchondroma versus chondrosarcoma in the appendicular skeleton: differentiating features. *Radiographics* 1998; **18**: 1213-37; quiz 1244-5 [PMID: 9747616 DOI: 10.1148/radiographics.18.5.9747616]
38 **Pannier S**, Legeai-Mallet L. Hereditary multiple exostoses and enchondromatosis. *Best Pract Res Clin Rheumatol* 2008; **22**: 45-54 [PMID: 18328980 DOI: 10.1016/j.berh.2007.12.004]
39 **Subhawong TK**, Winn A, Shemesh SS, Pretell-Mazzini J. F-18 FDG PET differentiation of benign from malignant chondroid neoplasms: a systematic review of the literature. *Skeletal Radiol* 2017; **46**: 1233-1239 [PMID: 28608242 DOI: 10.1007/s00256-017-2685-7]
40 **Kushchayeva YS**, Kushchayev SV, Glushko TY, Tella SH, Teytelboym OM, Collins MT, Boyce AM. Fibrous dysplasia for radiologists: beyond ground glass bone matrix. *Insights Imaging* 2018; **9**: 1035-1056 [PMID: 30484079 DOI: 10.1007/s13244-018-0666-6]
41 **Qu N**, Yao W, Cui X, Zhang H. Malignant transformation in monostotic fibrous dysplasia: clinical features, imaging features, outcomes in 10 patients, and review. *Medicine (Baltimore)* 2015; **94**: e369 [PMID: 25621678 DOI: 10.1097/MD.0000000000000369]
42 **Bernard SA**, Murphey MD, Flemming DJ, Kransdorf MJ. Improved differentiation of benign osteochondromas from secondary chondrosarcomas with standardized measurement of cartilage cap at CT and MR imaging. *Radiology* 2010; **255**: 857-865 [PMID: 20392983 DOI: 10.1148/radiol.10082120]
43 **Hadjipavlou A**, Lander P, Srolovitz H, Enker IP. Malignant transformation in Paget disease of bone. *Cancer* 1992; **70**: 2802-2808 [PMID: 1451058 DOI: 10.1002/1097-0142(19921215)70:12<2802::AID-CNCR2820701213>3.0.CO;2-N]
44 **Cabarrus MC**, Ambekar A, Lu Y, Link TM. MRI and CT of insufficiency fractures of the pelvis and the proximal femur. *AJR Am J Roentgenol* 2008; **191**: 995-1001 [PMID: 18806133 DOI: 10.2214/AJR.07.3714]
45 **Panteli M**, Puttaswamaiah R, Lowenberg DW, Giannoudis PV. Malignant transformation in chronic osteomyelitis: recognition and principles of management. *J Am Acad Orthop Surg* 2014; **22**: 586-594 [PMID: 25157040 DOI: 10.5435/JAAOS-22-09-586]
46 **Smith J**, Mello LF, Nogueira Neto NC, Meohas W, Pinto LW, Campos VA, Barcellos MG, Fiod NJ, Rezende JF, Cabral CE. Malignancy in chronic ulcers and scars of the leg (Marjolin's ulcer): a study of 21 patients. *Skeletal Radiol* 2001; **30**: 331-337 [PMID: 11465774 DOI: 10.1007/s002560100355]


Published By Baishideng Publishing Group Inc
7041 Koll Center Parkway, Suite 160, Pleasanton, CA 94566, USA
Telephone: +1-925-2238242
Fax: +1-925-2238243
E-mail: bpgoffice@wjgnet.com
Help Desk: https://www.f6publishing.com/helpdesk
https://www.wjgnet.com